

# Validation of Numerical Simulation for Subdural Cortical Stimulation

## Using Spherical Phantoms and Anatomically Realistic Head Phantom

Jinmo Jeong<sup>1</sup>, Donghyeon Kim<sup>2</sup>, Sangdo Jeong<sup>1</sup>, Jonghyun Lee<sup>1</sup>, Euiheon Chung<sup>1,3</sup>,  
Sung Chan Jun<sup>2</sup> and Sohee Kim<sup>1,3</sup>

<sup>1</sup>Department of Medical System Engineering, Gwangju Institute of Science and Technology, Gwangju, South Korea

<sup>2</sup>School of Information and Communications, Gwangju Institute of Science and Technology, Gwangju, South Korea

<sup>3</sup>School of Mechatronics, Gwangju Institute of Science and Technology, Gwangju, South Korea

**Keywords:** Cortical Stimulation, Numerical Simulation, Finite Element Method, Brain Phantom.

**Abstract:** The purpose of this study is to investigate the accuracy of numerical simulation for electric brain stimulation. For this, we modelled brains using simple computational models with 2 and 3 shells, with and without realistic head geometry, and performed numerical simulations using finite element method (FEM). The corresponding head phantoms were constructed for the validation of simulation results. We implanted stimulation electrodes in the head phantom, and measured the electric potential induced by the electrodes. When comparing the electric potential obtained from numerical simulations and phantom experiments, both results showed similar trend and amplitude, with a relative difference of 13.64% on average in the realistic head model study. This result demonstrates that predicting the electric potential and its gradient (current density) using computational simulation is reliable with reasonably small deviation from the actual measurement.

## 1 INTRODUCTION

Electric brain stimulation (EBS) is known to be useful in treating brain disorders: essential tremor, chronic stroke, chronic pain, Parkinson's disease, movement disorder, refractory epilepsy, depression, aphasia, and dystonia as an intervention therapy. Although EBS is gaining a potential to treat brain disorders and brain diseases, side effects (seizure (Bezard et al., 1999)) and mechanisms of EBS are obscure, and optimal stimulation parameters (electrode position, amplitude, waveform, and duration) remain unknown. Animal experiments and computational studies are essential to answer these questions. A computational study can provide the information for estimating the effect of brain stimulation by the implicit assumption that the excitability of neurons is linearly proportional to the magnitude of the current density (or electric field) in the brain. (Wongsarnpigoon and Grill, 2012; Manola et al., 2007) analysed the response of the neuron on invasive brain stimulation with various stimulation amplitudes and positions using a computational

brain model. (Opitz et al., 2013) generated an individual brain model and showed a positive correlation between fMRI and some simulation results. In general, computational simulation results are required to be validated. However, there have been few papers on the validation of simulations. (Wei and Grill 2005) built a phantom for the validation of deep brain stimulation and compared the simulation and phantom results. (Kim et al., 2010) investigated the effect of head model, conductivity condition, and position of stimulation numerically, and constructed a head phantom for verification. These studies made phantom models and compared them with simulation results. However, insufficient brain domain may lead to ignore unwanted side effects, and using oversimplified brain structures such as shell model or smoothed cortex model may not inform the precise effect of EBS.

The objective of this study is to investigate the accuracy of the simulation for EBS (more specifically subdural cortical stimulation (SuCS)). For the study, we modelled simple sphere models

based on 2- and 3-shells and constructed the corresponding head phantoms. Based on these models, we implanted stimulation electrodes in the head phantom, and measured the electric potential induced by the electrodes. In the phantom modelling, we used agarose/NaCl mixture to control the electric conductivity and the shape of head phantom. In addition, we made a computational brain model based on a geometry obtained from magnetic resonance imaging (MRI) and compared the simulation and phantom experimental results.

## 2 METHODS

As the purpose of this study is to validate the simulation for EBS, especially SuCS, the brain geometries for simulation and phantom model were identical. For comparison, we made 3 types of brain models (2 shells, 3 shells, and 3 shells with realistic brain geometry). We used similar isotropic conductivity that was measured through experiments in the human brain except the 2 shells model (Datta et al. 2009). Figure 1 shows the schematic view of each model.

### 2.1 Simulation Modelling

In general, EBS involves injecting into the brain the direct electrical current or induced current by voltage via electrode(s). Maxwell's equation explains such electrical behaviour within the brain; thus, the following Laplace equation governs the domain in our simulation model  $\Omega$ :

$$\nabla \cdot (\sigma \nabla V) = 0 \text{ in } \Omega \quad (1)$$

Here  $V$  and  $\sigma$  are an electrical potential and an electrical conductivity in  $\Omega$ , respectively. Assuming that the electric flux through out of model  $\Omega$  is negligibly small (that is, insulated), the Neumann boundary condition is applied on outer boundaries of the model as follows:

$$\mathbf{n} \cdot \mathbf{J} = 0 \text{ on } \partial\Omega_{\text{outer}} \quad (2)$$

where  $\mathbf{n}$  and  $\mathbf{J}$  are the normal vector to the boundary and the current density, respectively. Further, the Dirichlet boundary conditions are applied at the cathode electrode surface  $\psi_{\text{cathode}}$  in the model  $\Omega$  and anode electrode surface  $\psi_{\text{anode}}$  as follows:

$$V = 0 \text{ on } \partial\psi_{\text{cathode}} \quad (3)$$

$$V = V_0 \text{ on } \partial\psi_{\text{anode}} \quad (4)$$

where  $V_0$  is an input voltage magnitude. We applied simulation voltage  $V_0$  as 5V in the 2 and 3 shell

models. Also, 1V simulation voltage was applied in the 3 shell model with realistic brain geometry. To obtain the solution for this numerical problem, we used the finite element method (FEM). To solve the boundary value problem using FEM, volume mesh was generated in an adaptive way: we applied volume constraint factor to each model component, so that the mesh was coarse around simple structures, while a finer mesh was used around complex structures. The numbers of tetrahedron elements were 2,189,812 for 2 shells model, 2,154,260 for 3 shells model, 3,026,529 for 3 shells model with realistic brain geometry. The convergence of stimulation' results using finer model was verified as 2 shells: 0.0098%, 3 shells: 0.0056% and 3 shells with realistic brain: 1.9%. Bi-conjugate gradient stable solver with incomplete LU preconditioner was used as the solver. All simulations were done using COMSOL Multiphysics 4.3 (COMSOL Inc Burlingtonm, MA).

### 2.2 Phantom Design and Measurement

For the purpose of validating simulation results, we constructed the phantoms that correspond to each simulation model. For modelling Sphere phantoms, we used 'mold' to shape the model's geometry. Sphere based models (2 shells and 3 shells) were made using commercially available plastic sphere molds. To make a Sphere phantom with 2 and 3 shells, we assembled the phantom from inner layer to outer layer. At first, the two plastic sphere molds having different radius were prepared, then we filled the inner sphere mold using agarose/NaCl mixture.

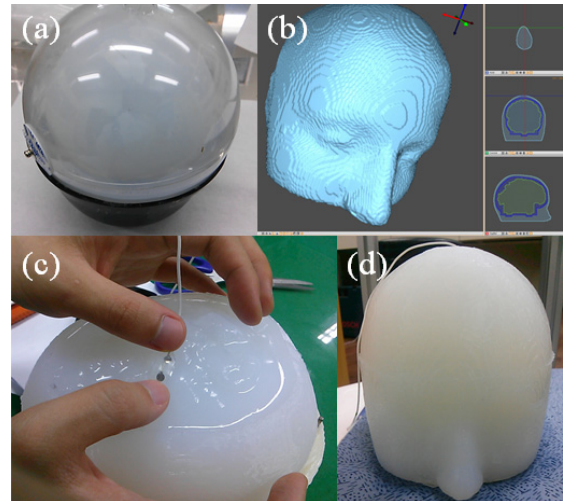


Figure 1: (a): Production process of the sphere phantom, (b): Schematic of assembled brain phantom, (c) location of the electrode, (d) The completed brain phantom.

After producing the inner layer, we put the mold of the next outer layer in position and then filled with agarose/NaCl mixture again. At second, we added the outermost layer using the other plastic sphere molds which is larger than other molds for make a 3 shells sphere phantom. Figure 1-(a) shows the process of assembling the sphere phantom. Also, as shown in Figure 1-(b), magnetic resonance images (MRI) of human brain were used to generate a mold for making the 3 shells model with realistic brain geometry. The MRI data was segmented as skin (3<sup>rd</sup> layer), skull and cerebrospinal fluid (CSF) (2<sup>nd</sup> layer), and gray matter and white matter (1<sup>st</sup> layer). Then based on the segmented data, we made the mold using a 3D printer (Inspire 3D Printer, A450). Figure 1 -(c, d) shows the model phantoms made of 3 shells and 3 shells with realistic brain geometry, respectively. We placed two stimulation electrodes for anode and cathode, respectively: the anode on one side of the sphere and the cathode on the opposite side of the first one. Especially, in the 3 shells model with realistic brain geometry, two stimulation electrodes were placed on motor cortex (figure 1-(c)) and a reference electrode was placed on bottom of the model. A 5[V] DC voltage was applied on each model using a function generator (Agilent, E3631A) and the voltage was measured by a digital multi-meter (Agilent, 34410A). Electric potentials induced by the electrodes implanted in the phantoms were measured at surface, 10mm depth, and 2cm depth of each phantom and the measuring points in 2 shells and 3 shells phantom was from 10° to 170° with 10° interval (figure 2-(a, b)). 3 shells model with realistic brain geometry had irregular sensing points and is shown in figure 2-c.

### 2.3 Conductivity of Phantom Material

One of the methods to assign the conductivity of the phantom is to adjust the NaCl concentration (mg/ml) in agarose since the electrical conductivity of agarose was controlled by changing the concentration of NaCl (Wongsarnpigoon and Grill 2012; Manola et al., 2007). In this study, powdered agarose (Affymetrix, Agarose - LE) and NaCl were mixed with deionized (DI) water. This solution including agarose (2.6mg/ml), NaCl (DUKSAN, Sodium Chloride) and DI water was stirred using a magnetic stir bar and poured into a regular hexahedron mold. The dimensions of the mold were 74 mm of length, 25 mm of width and 2.4 mm of length. The resistance of completed agarose/NaCl mixture was measured by an impedance measurement system (Gamry, Reference 600) for identifying the conductivity of agarose with NaCl, and then we calculated the conductivity using equation.

$$\sigma = \ell / (A \cdot \Omega) \quad (5)$$

Here  $\sigma$ ,  $\ell$ , and  $A$  is conductivity [S/m], length [m], and area [m<sup>2</sup>], respectively.  $\Omega$  is the measured resistance [ohm]. Thus, the ratio of NaCl concentration to agarose was estimated and adjusted to mimic the conductivity of the phantom similar to that of the human brain.

Table 1 shows the conductivities of each layer in the phantoms used in this study. The assigned conductivity for 2 shells was not like actual brain conductivity. However, the other models had similar isotropic conductivity that was measured through experiments in the human brain (Datta et al., 2009).

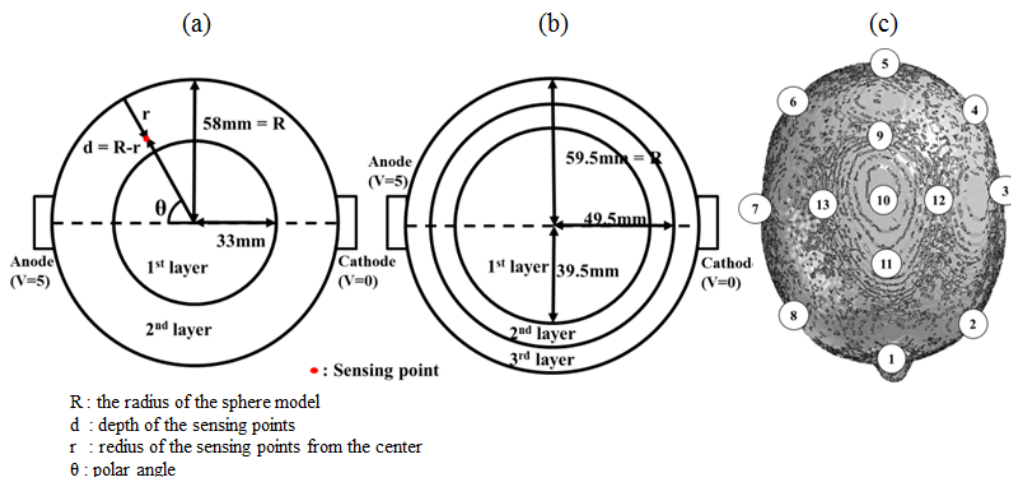


Figure 2: (a, b): Schematic view of 2 shells and 3 shells sphere phantom model, (c): Schematic view of brain phantom model. The numbers on (c) represents sensing points.

Table 1: The conductivity of each spherical phantom and simulation model (1<sup>st</sup> layer is central part).

	2 shells	3 shells
1 <sup>st</sup> layer	0.012 [S/m]	0.214 [S/m]
2 <sup>nd</sup> layer	0.28 [S/m]	0.012 [S/m]
3 <sup>rd</sup> layer	-	0.470 [S/m]

### 3 RESULTS

#### 3.1 Sphere Phantom Results versus Simulation Results

Figure 3-(a-c) shows the result of numerical simulation and phantom experiment using 2 shells sphere model. When we measured the electric potential with polar angles from 10° to 170° on a basis of the center of shells with 10° interval, the slope of electric potential was steep around the electrodes and flat far away from the electrodes. Also, there was small variation in electric potential when measured at points deep inside the brain model. Overall behaviour between simulation and phantom experiment were similar and the relative difference was quite low (4.68% on average). Even in the steepest area ( $\theta$ : 0~30°, d: 0~10mm), the phantom experimental result was in good agreement with the result of simulation. Furthermore, when a more complicated 3-shells brain model was used, we

could see a relative difference of 7.18% on average between the simulation and experimental results, obtained at 3 different depths, as shown in figure 3-(d-f). When comparing the simulation results of 2 shells and 3 shells sphere models, there was a difference in magnitude of electric potential of 0.21[V] on average. However, they showed the same shape of curve. The difference between the result of simulation and phantom experiment was within 8.82%.

#### 3.2 Realistic Head Results versus Simulation Results

Figure 4 shows the electric potential at 13 different points on surface of the head model, 10mm depth, and 20mm depth obtained from the simulation and phantom experiment. Most of the electric potential from both simulation and experimental results was around 0.87[V]. Also, from simulation, the electric potential in the upper area of model (around implanted electrodes; sensing point 9, 10, 11, 12, and 13) was higher, 0.90[V] on average, when compared to other measurement points where 0.86[V] on average was obtained. From phantom experiment, however, the potentials at point 11, 12, and 13 were below the average potential: potential at point 11 was 0.86[V], 0.81[V] at point 12, and 0.84[V] at point 13 while the average potential was 0.87[V] along the depth). The average relative

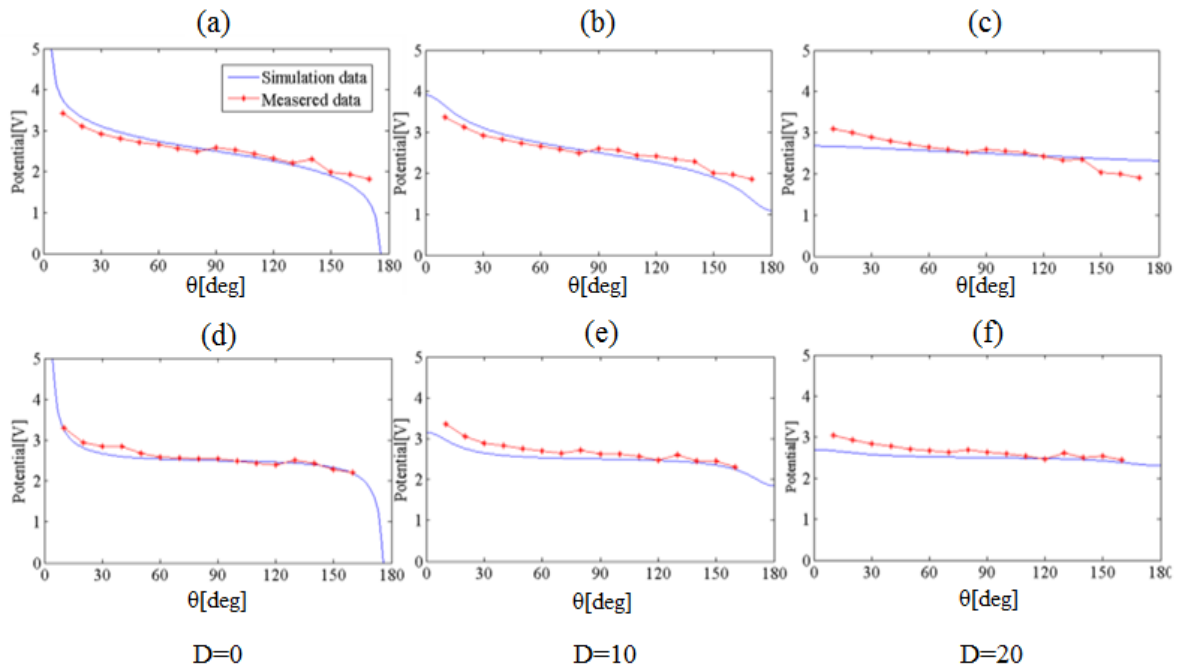


Figure 3 Above: Results of the comparative experiment using 2 shells sphere model, (a): surface (b): 10mm (c): 20mm, Below: Results of the comparative experiment using 3 shells sphere model, (d): surface (e): 10mm (f): 20mm.

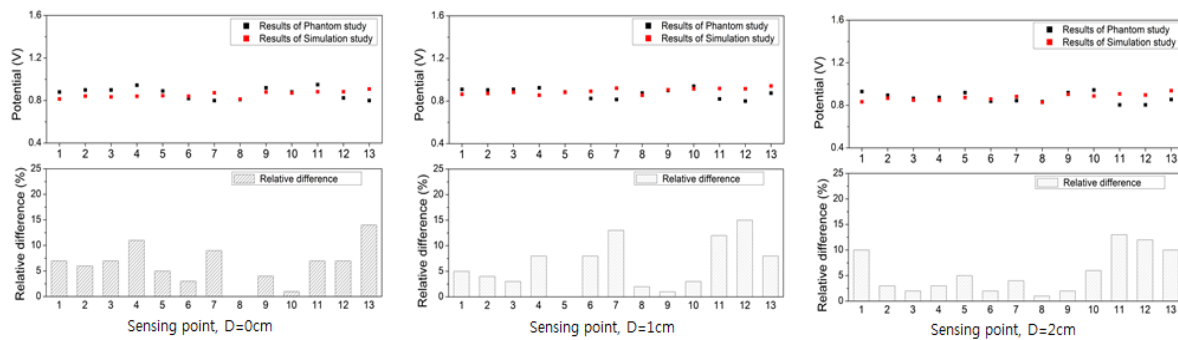


Figure 4: Results of the comparative experiment using brain model, (a): surface (b): 10mm (c): 20 mm.

difference between the results was 6.02%. Relatively higher differences were observed at the points 11, 12, and 13: 10.60%, 11.03%, and 10.33% on average with depth, respectively. When considering relative difference with respect to the depth of measurement, there was little difference among the potentials obtained at different depths (surface: 6.23%; 10mm: 5.57%; 3cm: 6.19%).

#### 4 DISCUSSION

We performed a number of brain phantom studies to evaluate the accuracy of numerical simulation for EBS. All the results (2 and 3 layer sphere models, and 3 shells with realistic head geometry) showed good agreements in electric potential between simulation and phantom experiments (average relative difference: 4.57% in 2 shells; 7.09% in 3 shells; 6.03% in 3 shells with realistic geometry) and the trend of voltage between simulation and phantom study was similar among results.

In relative difference view, it was low at between electrodes and high at around anode and cathode (around anode: 8.43%, between electrodes: 4.10%, and around cathode: 9.85% in average with models and depth) when we examined the relative difference between simulation and experiment according to different measurement points in 2 shells and 3 shells models (polar angles: from 0° to 30°, between electrodes: 40° to 140°, around cathode: 150° to 180°). Also, these differences are even seen in the 3 shells model with realistic brain geometry. From the result of simulation using 3 shells with realistic brain geometry, we could see the higher potential at point 9, 10, 11, 12, and 13 because of its position and these points have higher relative difference than the other points. Although, there was little difference between simulation and phantom experimental results, there were several limitations for validating

simulation results. First, due to a small displacement of measuring point, there was a larger relative difference around electrode. So far, there are reports which tried to measure electric potential on phantom. However, they reported the accuracy of measured electric potential was not good because of poor spatial control over placement of the measuring sensor (Jung et al., 2013; Suesserman et al., 1991). To overcome the problem, coordinate-based measuring machine is needed. As well, generated water screen arising in the phantom model due to solidification of agarose/NaCl mixture has another possibility for the difference between the simulation and experimental results. Second, in the 3 shells with realistic geometry phantom, the variation of electric potential at sensing point evaluated by numerical stimulation was not big; also the variation of electric potential at sensing point measured by phantom was not big. Both results mean that we chose measuring sensing points having similar electrical potential. To compare the both results as aspect of validation for result of simulation, choice the sensing points set which having big variance is very important. As a further study, thus, we are working on the measurements with the realistic head phantom focusing on the vicinity of stimulation electrodes where the gradient of potential is large as the target region of stimulation is generally near stimulation electrode. Furthermore similar phantom study with varying dynamic voltage or current instead of applying static voltage or current would provide more insight into the realistic electrical stimulation practice.

#### 5 CONCLUSIONS

In this paper, we systematically compared numerical simulation and experimental phantom results to validate simulation tools for subdural cortical

stimulation. Based on our results, we could see good agreements between simulated and measured electrical potential in both simple spherical phantom and realistic head phantom experiments. These results provide a convincing justification for investigating the effects of EBS using computational models.

## ACKNOWLEDGEMENTS

This work was supported by the Institute of Medical System Engineering (iMSE) in the GIST.

## REFERENCES

- Bezard, E. et al., 1999. Cortical Stimulation and Epileptic Seizure: A Study of the Potential Risk in Primates. *Neurosurgery*, 45(2).
- Datta, A. et al., 2009. Gyri -precise head model of transcranial DC stimulation: Improved spatial focality using a ring electrode versus conventional rectangular pad. *Brain stimulation*, 2(4), pp.201–207.
- Jung, Y. et al., 2013. An image-guided transcranial direct current stimulation system: a pilot phantom study. *Physiological measurement*, 937.
- Kim, D.-H. et al., 2010. Distortion of the electric field distribution induced in the brain during transcranial magnetic stimulation. *IET Science, Measurement & Technology*, 4(1), p.12.
- Manola, L. et al., 2007. Anodal vs cathodal stimulation of motor cortex: A modeling study. *Clinical Neurophysiology*, 118(2), pp.464–474.
- Opitz, A. et al., 2013. Physiological observations validate finite element models for estimating subject-specific electric field distributions induced by transcranial magnetic stimulation of the human motor cortex. *NeuroImage*, 81, pp.253–64.
- Suesserman, M. F., Spelman, F. a & Rubinstein, J.T., 1991. In vitro measurement and characterization of current density profiles produced by non-recessed, simple recessed, and radially varying recessed stimulating electrodes. *IEEE transactions on bio-medical engineering*, 38(5), pp.401–8.
- Wei, X. F. & Grill, W. M., 2005. Current density distributions, field distributions and impedance analysis of segmented deep brain stimulation electrodes. *Journal of neural engineering*, 2(4), pp.139–47.
- Wongsarnpigoon, A. & Grill, W. M., 2012. Computer-based model of epidural motor cortex stimulation: effects of electrode position and geometry on activation of cortical neurons. *Clinical neurophysiology: official journal of the International Federation of Clinical Neurophysiology*, 123(1), pp.160–72.